International Journal of Engineering Research & Technology (IJERT)
ISSN: 2278-0181
Vol. 1 Issue 10, December- 2012

Modelling and Simulation of Matrix Converter fed Induction Motor Drive using PID control

Abhijit Mandal
M.E.(Power Electronics) Student
Raipur Institute of Technology,
Raipur(C.G.), India

Manoj Kumar Nigam
Reader, Department of Electrical Engineering
Raipur Institute of Technology,
Raipur(C.G.), India

IJERT

Abstract

This paper presents modelling and simulation of matrix converter using PID control scheme for controlling the induction motor drive. Simulation model consists a three phase matrix converter, an induction motor, a field oriented controller and a power supply. Venturini's modulation algorithm is used for simulation model. The algorithm of Venturini provides unity displacement factor in the input regardless of the load displacement factor and it can be easily implemented in the closed loop operation. Simulation results are presented for the output of converter. The result shows that the performance of matrix converter fed induction motor drive improved by using PID controlling scheme.

Index Terms: Matrix Converter, Induction Motor, Field oriented control, PID control

1. Introduction

Matrix Converter is the most popular converter in a.c. to a.c. direct converter family and generally used in industrial applications. The a.c. to a.c. matrix converter was first investigated by Gyugyi and Pelly in 1976 [1]. Venturini and Alesina have introduced a matrix converter design using a generalized high frequency switching strategy [2]. During recent years, the matrix converter has entered the power electronics industry but only a few of practical matrix converters have been designed.

The matrix converter has become popular because of its simple topology, absence of large dc link capacitor and easy control of input power factor. Matrix converter fulfils the requirements to provide a sinusoidal voltage at the load side and, on the other hand, it is possible to adjust the unity power factor on the mains side under certain conditions [3]. Since there is no d.c. link as in common converters, the matrix converter can be built as a full-silicon structure. However , a main filter is necessary to smooth the pulsed currents on the input side of the matrix converter. Using a sufficiently high pulse frequency, the output voltage and current both are shaped sinusoidaly. The matrix converter is an alternative to a inverter drive for three-phase frequency control.

The converter consists of nine bi-directional switches. Each of these bi-directional switches can be constructed by power semiconductor devices as shown in Fig. 2. Traditionally, two IGBTs with anti-paralleled diodes are connected in series to construct one bi-directional switch (Fig. 2a). However, this structure requires 18 IGBTs and 18 diodes, resulting in much more power loss than in conventional AC-DC-AC converters and hindering the further popularization of the matrix converter. Newly developed IGBT with reverse blocking capability (RB-IGBT) helps to resolve this problem. A bi-directional switch is realized by a simple placing of two RB-IGBTs in anti-parallel while 18 diodes used for blocking the voltage in matrix converter are no longer required (Fig. 2b).

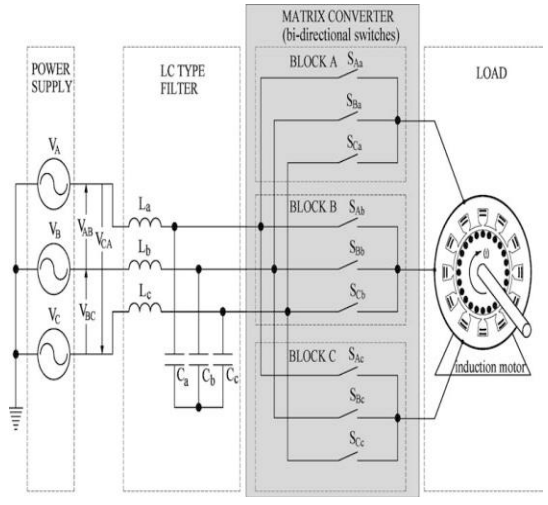

Fig. 1 Matrix converter schematic block diagram representation

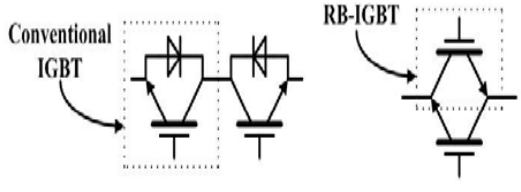

Fig. 2. Different structures of bi-directional power switches: (a) Conventional IGBTs with diodes (b) RB-IGBTs

switches, arranged as three sets of three so that any of the three input phases can be connected to any of the three output lines, as shown in Fig. 1, where uppercase and lowercase letters are used to denote the input and output, respectively. The switches are then controlled in such a way that the average output voltages are a three-phase set of sinusoids of the required frequency and magnitude [4]. The matrix converter can comply with four quadrants of motor operations, while generating no higher harmonics in the three-phase a.c. power supply. Compared with conventional drives, there is potential for reduced cost of manufacture and maintenance, and increased power/weight and power/volume ratios. The circuit is inherently capable of bi-directional power flow and also offers virtually sinusoidal input current, without the harmonics usually associated with present commercial inverters. The physical realization of the matrix converter is not straightforward, due to the fact that there are no freewheeling paths. In addition, the number of devices in the power circuit is high compared with that in the inverter (for instance 18 switches and 18 diodes). Consequently, the timing of the switch actuation signals is particularly critical, and protection of the circuit under fault conditions requires very careful consideration [5].

2. Algorithm of Matrix Converter

A simplified version of the Venturini algorithm is used in this work [6]. This algorithm is defined in terms of the three-phase input and output voltages at each sampling instant and is convenient for closed loop operations. For the real-time implementation of the proposed modulation algorithm, it is required to measure any two of three input line-to-line voltages. Then, V_{im} and $\omega_i t$ are calculated as

$$V_{\text{im}}^2 = \tfrac{4}{9}(v_{AB}^2 + v_{BC}^2 + v_{AB}v_{BC}) \quad (1)$$

$$\omega_i t = \arctan\left(\frac{v_{BC}}{\sqrt{3}\left(\frac{2}{3}v_{AB} + \frac{1}{3}v_{BC}\right)}\right) \quad (2)$$

where v_{AB},v_{BC} are the instantaneous input line voltages. The target output peak voltage and the output position are calculated as

$$V_{\text{om}}^2 = \tfrac{2}{3}(v_a^2 + v_b^2 + v_c^2) \quad (3)$$

$$\omega_o t = \arctan\left(\frac{v_b - v_c}{\sqrt{3}v_a}\right) \quad (4)$$

where v_a, v_b, v_c are the target phase output voltages. Alternatively, in a closed loop system (for example a field-oriented controlled drive), the voltage magnitude and angle may be direct outputs of the control loop.

Then, the voltage ratio is calculated

$$q = \sqrt{\frac{V_{\text{om}}^2}{V_{\text{im}}^2}} \quad (5)$$

where q is the desired voltage ratio, and V_{im} is the peak input voltage.

Triple harmonic terms are found

$$K_{31} = \frac{2}{9}\frac{q}{q_{\text{m}}}\sin(\omega_i t)\sin(3\omega_i t) \quad (6)$$

$$K_{32} = \frac{2}{9}\frac{q}{q_{\text{m}}}\sin\left(\omega_i t - \frac{2\pi}{3}\right)\sin(3\omega_i t) \quad (7)$$

$$K_{33} = -\sqrt{V_{\text{om}}^2}\left[\frac{1}{6}\cos(3\omega_o t) - \frac{1}{4}\frac{1}{q_{\text{m}}}\cos(3\omega_i t)\right] \quad (8)$$

where q_m is the maximum voltage ratio (0.866).

Then, the three modulation functions for output phase a are given as

IJERT

$$M_{Aa} = \tfrac{1}{3} + k_{31} + \frac{2}{3V_{\text{im}}^2}(v_a + k_{33})\left(\tfrac{2}{3}v_{AB} + \tfrac{1}{3}v_{BC}\right) \quad (9)$$

$$M_{Ba} = \frac{1}{3} + k_{32} + \frac{2}{3V_{\text{im}}^2}(v_a + k_{33})\left(\tfrac{1}{3}v_{BC} - \tfrac{1}{3}v_{AB}\right) \quad (10)$$

$$M_{Ca} = 1 - (M_{Aa} + M_{Ba}) \quad (11)$$

The modulation functions for the other two output phases, b and c are obtained by replacing v_b and v_c with v_a, respectively in Equations (9) and (10). Note that the modulation functions have third harmonic components at the input and output frequencies added to them to produce output voltage, v_o. This is a requirement to get the maximum possible voltage ratio [3]. It should be noted that in Eq. (3) there is no requirement for the target outputs to be sinusoidal. In general, three phase output voltages and input currents can be defined in terms of the modulation functions in matrix form as

$$v_{\text{oph}} = M v_{\text{iph}}$$
$$\begin{bmatrix} v_a \\ v_b \\ v_c \end{bmatrix} = \begin{bmatrix} M_{Aa} & M_{Ba} & M_{Ca} \\ M_{Ab} & M_{Bb} & M_{Cb} \\ M_{Ac} & M_{Bc} & M_{Cc} \end{bmatrix} \begin{bmatrix} v_A \\ v_B \\ v_C \end{bmatrix} \quad (12)$$

$$i_{\text{iph}} = M^{\text{T}} i_{\text{oph}}$$
$$\begin{bmatrix} i_A \\ i_B \\ i_C \end{bmatrix} = \begin{bmatrix} M_{Aa} & M_{Ab} & M_{Ac} \\ M_{Ba} & M_{Bb} & M_{Bc} \\ M_{Ca} & M_{Cb} & M_{Cc} \end{bmatrix} \begin{bmatrix} i_a \\ i_b \\ i_c \end{bmatrix} \quad (13)$$

where the superscript T denotes a transpose, and M is the instantaneous input-phase to output-phase transfer matrix of the three-phase matrix converter. v_{iph} and v_{oph} are the input and output phase voltage vectors, and i_{iph} and i_{oph} represent the input and output phase current vectors. Alternatively, from Equations (12) and (13), the output-line voltages and input-line currents can be expressed as

$$v_{\text{oLine}} = m v_{\text{iLine}}$$
$$\begin{bmatrix} v_{ab} \\ v_{bc} \\ v_{ca} \end{bmatrix} = \begin{bmatrix} m_{Ab} & m_{Bb} & m_{Cb} \\ m_{Ac} & m_{Bc} & m_{Cc} \\ m_{Aa} & m_{Ba} & m_{Ca} \end{bmatrix} \begin{bmatrix} v_{AB} \\ v_{BC} \\ v_{CA} \end{bmatrix} \quad (14)$$

$$i_{\text{iLine}} = m^{\text{T}} i_{\text{oLine}}$$
$$\begin{bmatrix} i_{AB} \\ i_{BC} \\ i_{CA} \end{bmatrix} = \begin{bmatrix} m_{Ab} & m_{Ac} & m_{Aa} \\ m_{Bb} & m_{Bc} & m_{Ba} \\ m_{Cb} & m_{Cc} & m_{Ca} \end{bmatrix} \begin{bmatrix} i_{ab} \\ i_{bc} \\ i_{ca} \end{bmatrix} \quad (15)$$

where

$$\begin{aligned}
m_{Ab} &= \tfrac{1}{3}(M_{Aa} - M_{Ab}) - \tfrac{1}{3}(M_{Ba} - M_{Bb}) \\
m_{Bb} &= \tfrac{1}{3}(M_{Ba} - M_{Bb}) - \tfrac{1}{3}(M_{Ca} - M_{Cb}) \\
m_{Cb} &= \tfrac{1}{3}(M_{Ca} - M_{Cb}) - \tfrac{1}{3}(M_{Aa} - M_{Ab}) \\
m_{Ac} &= \tfrac{1}{3}(M_{Ab} - M_{Ac}) - \tfrac{1}{3}(M_{Bb} - M_{Bc}) \\
m_{Bc} &= \tfrac{1}{3}(M_{Bb} - M_{Bc}) - \tfrac{1}{3}(M_{Cb} - M_{Cc}) \\
m_{Cc} &= \tfrac{1}{3}(M_{Cb} - M_{Cc}) - \tfrac{1}{3}(M_{Ab} - M_{Ac}) \\
m_{Aa} &= \tfrac{1}{3}(M_{Ac} - M_{Aa}) - \tfrac{1}{3}(M_{Bc} - M_{Ba}) \\
m_{Ba} &= \tfrac{1}{3}(M_{Bc} - M_{Ba}) - \tfrac{1}{3}(M_{Cc} - M_{Ca}) \\
m_{Ca} &= \tfrac{1}{3}(M_{Cc} - M_{Ca}) - \tfrac{1}{3}(M_{Ac} - M_{Aa})
\end{aligned} \quad (16)$$

3. Field Oriented Controller

The field-oriented control strategy was implemented in the matrix converter induction motor drive. The induction machine is controlled in synchronously rotating d–q axis frame with the d axis oriented along the stator flux vector position. In this way, a decoupled control between the electrical torque and the rotor excitation current is obtained. The indirect field oriented control technique using impressed voltages and control of field and torque current components was implemented in the drive system. The control requires the measurements of the stator currents and the rotor position. Equations (17), (18), and (19) are the fundamental equations for field-oriented control [13], and allow the induction motor to act like a separately excited d.c. machine with decoupled control of torque and flux, making it possible to operate the induction motor as a high-performance four-quadrant servo drive.

$$i_{\text{sd}} = \tau_{\text{r}} \frac{\text{d}i_{\text{mrd}}}{\text{d}t} + i_{\text{mrd}} \quad (17)$$

$$\omega_{\text{sl}} = \left(\frac{1}{\tau_{\text{r}} i_{\text{mrd}}}\right) i_{\text{sq}} \quad (18)$$

$$T_{\text{e}} = 3\left(\frac{P}{2}\right)\frac{L_0^2}{L_{\text{r}}} i_{\text{sd}} i_{\text{sq}} \quad (19)$$

Figure 3 shows a schematic block diagram for the field-oriented controlled matrix converter induction motor drive where three output currents and rotor position are required to be measured. The field-oriented control method shown in Fig. 3 imposes a rotor flux vector angle Θe which is aligned to the d axis. The motor speed, ω_r is measured and compared with the demanded speed ω_{r*}. The resulting speed error is then processed by a proportional-integral derivative (PID) controller to produce an i_{sq*} demand, which in the constant torque region is proportional to the torque demand, providing that the system is field-oriented. The flux current demand is maintained constant at just under saturation

IJERT

level when the machine runs below synchronous speed. However, field weakening must be introduced above synchronous speed at base frequency operating conditions so that the flux current reference is reduced as the speed is increased above its synchronous base.

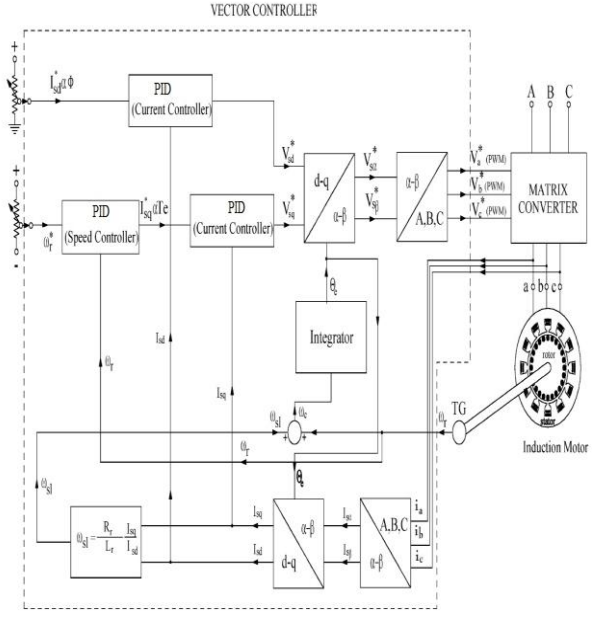

Fig. 3. Block diagram for vector controlled matrix converter induction motor drive.

The transformation of the instantaneous stator currents into field-oriented d and q axis components is carried out in two stages. First, the three instantaneous currents $i_{sa}(t)$, $i_{sb}(t)$, and $i_{sc}(t)$ are transformed to the stationary two axis currents, $i_{sa}(t)$ and $i_{sb}(t)$. These are then transformed into the rotating d–q axis currents, i_{sd} and i_{sq}. The equivalent complex operator $e^{-j\Theta e}$ is used in this transformation. Θe denotes the instantaneous flux vector angle, which is determined by summing the rotor position signal and the commanded slip position obtained by integrating Eq. (18). The inverse transformation of d and q axis values to the instantaneous stator reference frame is represented by the complex operator $e^{-j\Theta e}$. The two current controllers which employ PID control process the i_{sd} and i_{sq} errors to give V'_{sd} and V'_{sq}. Voltage compensation terms are added to the output of each current controller to get the resulting voltage reference signals V_{sd^*} and V_{sq^*}. These voltages are then converted to the three-phase voltages using the complex operator $e^{-j\Theta e}$. The three-phase voltages V_{a^*},V_{b^*}, V_{c^*}, and instantaneous flux vector angle Θe are used as the input signals for the Venturini algorithm (Equations. 1, 2, 3, 4, 5, 6, 7, 8, 9, 10, 11) to generate the duty cycles for each switch in the matrix converter.

4. d-q Model of Induction Motor

The simulation equations for an induction motor in the d–q synchronously rotating reference frame are given as [7]

$$\begin{bmatrix} V_{sq} \\ V_{sd} \\ 0 \\ 0 \end{bmatrix} = \begin{bmatrix} R_s & 0 & 0 & 0 \\ 0 & R_s & 0 & 0 \\ 0 & 0 & R_r & 0 \\ 0 & 0 & 0 & R_r \end{bmatrix} \begin{bmatrix} I_{sq} \\ I_{sd} \\ I_{rq} \\ I_{rd} \end{bmatrix} + \begin{bmatrix} p & \omega_s & 0 & 0 \\ -\omega_s & p & 0 & 0 \\ 0 & 0 & p & (\omega_s - \omega_r) \\ 0 & 0 & -(\omega_s - \omega_r) & p \end{bmatrix} \begin{bmatrix} \psi_{sq} \\ \psi_{sd} \\ \psi_{rq} \\ \psi_{rd} \end{bmatrix} \quad (20)$$

$$\begin{bmatrix} \psi_{sq} \\ \psi_{sd} \\ \psi_{rq} \\ \psi_{rd} \end{bmatrix} = \begin{bmatrix} L_s & 0 & L_o & 0 \\ 0 & L_s & 0 & L_o \\ L_o & 0 & L_r & 0 \\ 0 & L_o & 0 & L_r \end{bmatrix} \begin{bmatrix} I_{sq} \\ I_{sd} \\ I_{rq} \\ I_{rd} \end{bmatrix} \quad (21)$$

$$L_s = L_{ls} + L_o \qquad L_r = L_{lr} + L_o \quad (22)$$

$$T_e = 3\frac{P}{2}\frac{L_o}{L_r}(I_{sq}\psi_{rd} - I_{sd}\psi_{rq}) \quad (23)$$

$$J\frac{d\omega_{mech}}{dt} = T_e - T_L - f_v\omega_{mech} \quad (24)$$

where quantities with subscript q or d denote q axis or d axis quantities and quantities with subscript s or r denote stator or rotor quantities. Ψ denotes flux linkage, R is resistance, L_{ls} and L_{lr} are the stator and rotor leakage inductances, respectively, and L_o is the magnetizing inductance. L_s and L_r denote the self inductances of the stator and rotor, respectively. T_e and T_L are the motor torque and load torque, respectively. P is the number of poles, and f_v is the friction constant coefficient. J is inertia and ω_{mech} is the mechanical speed of the motor. All rotor quantities are referred to the stator.

5. Simulink Model

The simulation program constructed in Matlab/Simulink software package [8] comprises three main part switch are the matrix converter, induction motor, and field-oriented controller. Some subpart simulink diagrams of the main simulink model of

IJERT

matrix converter fed induction motor drive using PID are given below:

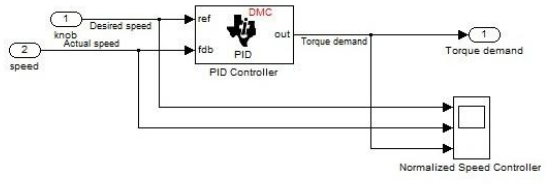

Fig. 4. Simulink diagram of speed controller

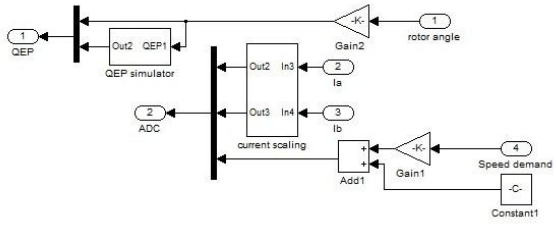

Fig. 5. Simulink diagram of motor output scaling

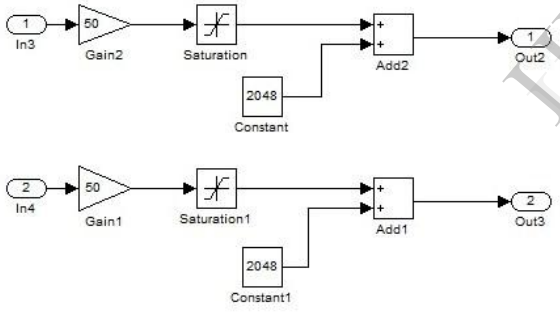

Fig. 6. Simulink diagram of current scaling

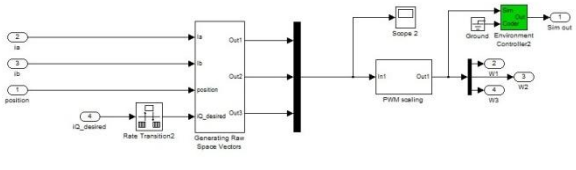

Fig. 7. Simulink diagram of generating space vector

6. Simulation Results

Simulation of the matrix converter fed induction motor using PID controller was performed for various operating conditions. Simulation results of various parameters are shown below:

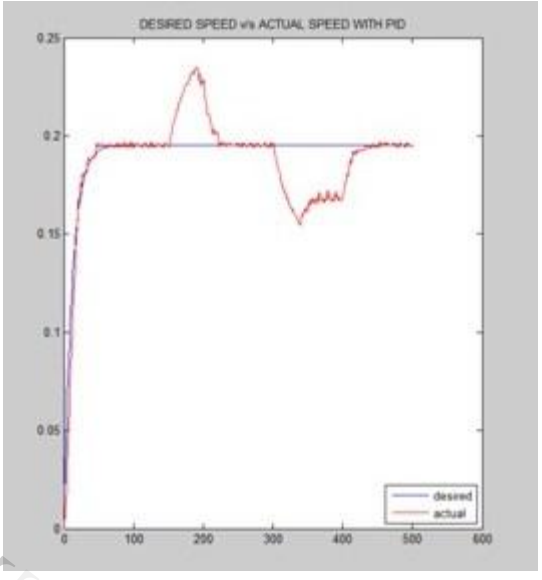

Fig.8. Variation between desired speed v/s actual speed

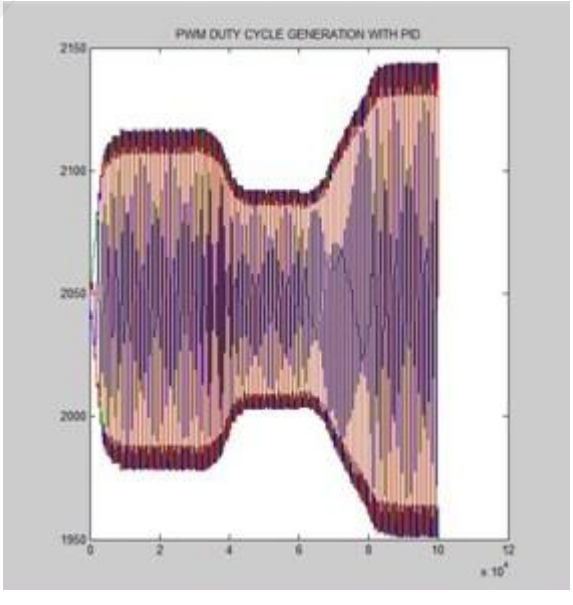

Fig. 9. PWM Duty Cycle

Figure 8 shows the variation between desired and actual speed of induction motor. In this figure blue lie

IJERT

shows the desired speed whereas red line shows actual speed of induction motor in practical condition.

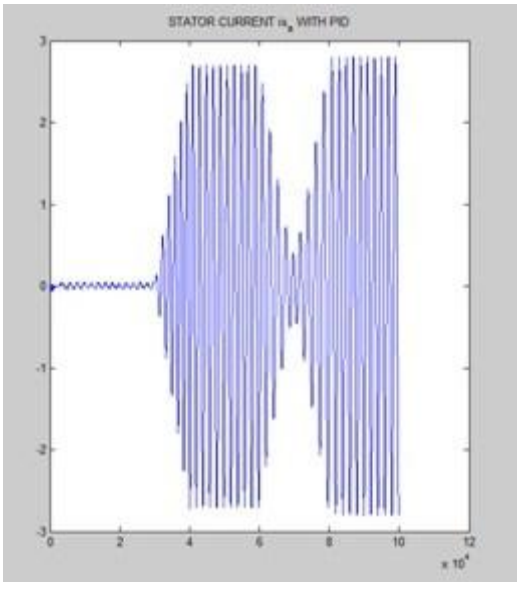

Fig. 10. Stator current of induction motor

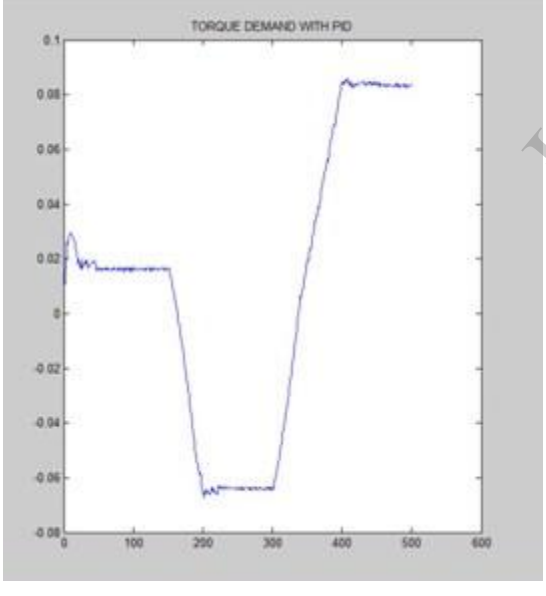

Fig. 11. Torque demand

Figure 9, 10, 11 shows the simulation results of PWM duty cycle, stator current, torque demand for matrix converter fed induction motor drive using PID controller.

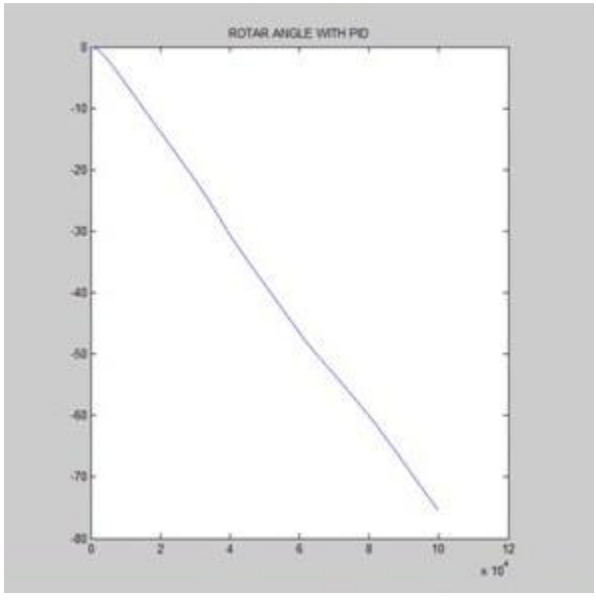

Fig. 12. Rotor angle of induction motor

IJERT

7. Conclusion

In this paper, a modelling and simulation study of the matrix converter-fed induction motor drive using PID control was carried out. A high-performance vector controlled drive employing the matrix converter was presented. Instead of the inverter with a d.c. link in the vector-controlled drive system, the use of the matrix converter made the drive system capable of operating in all four-quadrant regions. It was demonstrated that the matrix converter is capable of operating with unity input displacement factor regardless of the load power factor at the output. The simulation results shows that the performance of the motor drive system improved.

8. References

[1] L.Gyugi and B.R.Pelly, Static Power Freuency Changers, New York : Wiley-Interscience 1976.

[2] A.Alesina and M.Venturini,"Solid state power conversion : A Fourier analysis approach to generalized transformer synthesis" IEEE Transaction on Circuit systems, Vol. CAS-28, No.4, 1981, pp 319-330.

[3] Venturini M(1980) A new sine wave in sine wave out conversion technique which eliminates reactive elements In: proceedings of Powercon 7, San Diego, Calif., pp E3-1, E3-15.

[4] Alesina A, Venturini M (1981) Solid-state power conversion: a Fourier analysis approach to generalized transformer synthesis. Proc IEEE Trans Circuit Syst 28:319–330

[5] Empringham L, Wheeler PW, Clare JC(1998) Intelligent communication of matrix converter bidirectional switch cells using novel gate drive techniques In: IEEE PESC '98 Fukuoka, Japan, 17-22 May, Piscataway, N.J.,pp 707-713

[6] Su¨nter S (1995) A vector controlled matrix converter induction motor drive. PhD Thesis, Department of Electrical and Electronic Engineering, University of Nottingham.

[7] Krause PC, Thomas CH (1965) Simulation of symmetrical induction machinery. Proc IEEE Trans Power Apparatus Syst 84:1038–1053

[8] Math Works (2009) MATLAB_ for Microsoft Windows. Math Works, Mass.

[9] Chang J, Sun T, Wang A (2002) Highly compact AC–AC converter achieving a high voltage transfer ratio. Proc IEEE Trans Ind Electron 49:345–352

[10] Klumpner C, Nielson P, Boldea I, Blaabjerg F (2002) A new matrix converter motor (MCM) for industry applications. Proc IEEE Trans Ind Electron 49:325–335

[11] H. Altun and S. Sunter, "Matrix converter induction motor drive: modeling, simulation and control" Electrical Engineering (2003) 86: 25–33 DOI 10.1007/s00202-003 0179-1 Springer-Verlag 2003

[12] Yang Mei∗ , Kai Sun, Daning Zhou, Lipei Huang, and Xuansan Cai, "Novel improvements for matrix converter fed adjustable speed drive system", HAIT Journal of Science and Engineering, Volume 2, Issues 5-6

[13] Simon O, Mahlein J, Muenzer MN, Bruckmann M (2002) Modern solutions for industrial matrix-converter applications. Proc IEEE Trans Ind Electron 49:401–406

[14] Sunter S, Altun H, Clare JC (2002) A control technique for compensating the effects of input voltage variations on matrix converter modulation algorithms. Electric Power Components Syst 30:807–822

IJERT